Carbon Nanotubes as Photoacoustic Molecular Imaging Agents in Living Mice

Adam de la Zerda[1,2], Cristina Zavaleta[1], Shay Keren[1], Srikant Vaithilingam[2], Sunil Bodapati[1], Zhuang Liu[3], Jelena Levi[1], Bryan R. Smith[1], Te-Jen Ma[2], Omer Oralkan[2], Zhen Cheng[1], Xiaoyuan Chen[1], Hongjie Dai[3], Butrus T. Khuri-Yakub[2], Sanjiv S. Gambhir[1,4]

Supplementary Information

[1]Molecular Imaging Program at Stanford, Department of Radiology and Bio-X Program, the [2]Department of Electrical Engineering, the [3]Department of Chemistry and the [4]Department of Bioengineering, Stanford University, Palo Alto, CA 94305, USA.
e-mail: sgambhir@stanford.edu

© 2008 Macmillan Publishers Limited. All rights reserved.

Supplementary Figures

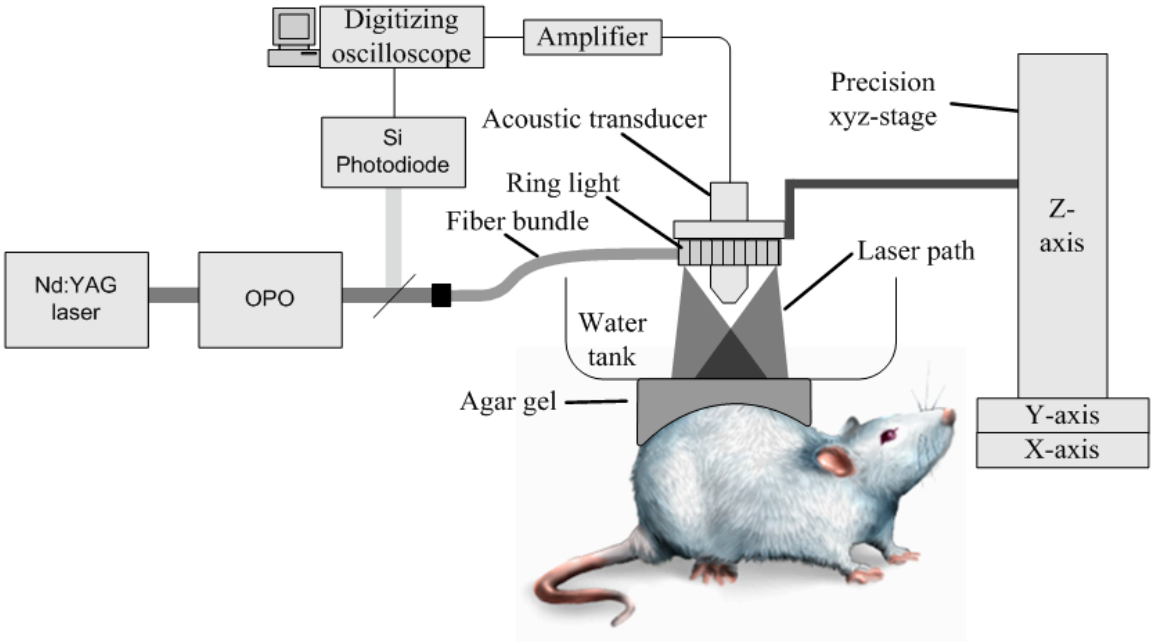

Supplementary Figure 1 Photoacoustic imaging instrument. A tunable pulsed laser (Nd:YAG laser and OPO) illuminated the subject through a fiber optic ring light. The photoacoustic signals produced by the sample were acquired using a 5 MHz focused transducer. A precision xyz-stage was used to move the transducer and the fiber ring along a planar 2D trajectory. The time of arrival and the intensity of the laser pulses were recorded using a silicon photodiode. This information was used to synchronize the acquisition and compensate for pulse-to-pulse variations in laser intensity. The analog photoacoustic signals were amplified using a 40 dB preamplifier and digitized using an oscilloscope.

© 2008 Macmillan Publishers Limited. All rights reserved.

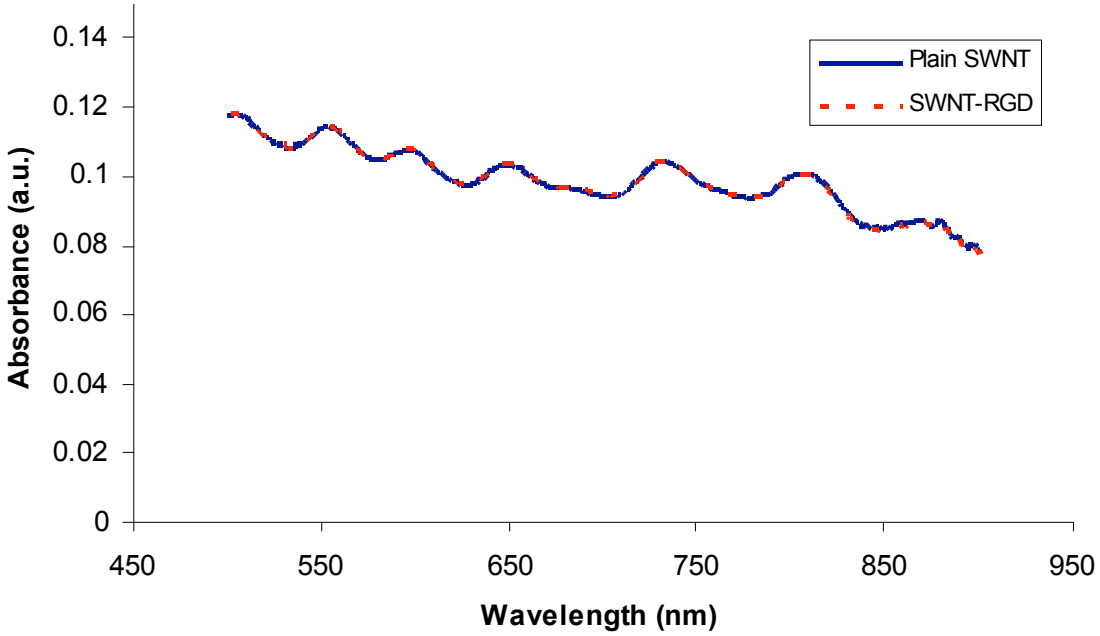

Supplementary Figure 2 Optical absorbance of SWNTs. The optical absorbance spectra of plain SWNTs (solid blue) and SWNT-RGD (dashed red) were measured from 500-900 nm. The spectra suggest that the RGD peptide conjugation does not perturb the optical properties of the SWNT.

Supplementary Notes

Cell uptake studies

We exposed SWNT-RGD to U87MG cells that express $\alpha_v\beta_3$ integrin on their surface for 30 min. Control studies included U87MG cells exposed to either plain SWNT or saline and HT-29 cells, which do not express $\alpha_v\beta_3$ integrin on their surface, exposed to SWNT-RGD. After exposure, the cells were washed with saline to remove unbound SWNTs and scanned *ex-vivo* using a Raman microscope. SWNTs produce a very unique Raman signal[1], allowing a Raman microscope to detect low concentrations of SWNTs in cells. U87MG cells that were exposed to SWNT-RGD were found to have 75% higher signal than U87MG cells exposed to plain SWNT ($p < 0.05$) and 195% higher signal than HT-

© 2008 Macmillan Publishers Limited. All rights reserved.

29 cells exposed to SWNT-RGD ($p < 0.05$). Cells exposed to saline only showed negligible signal compared to any of the groups ($p < 0.05$) (**Supplementary Figure 3**).

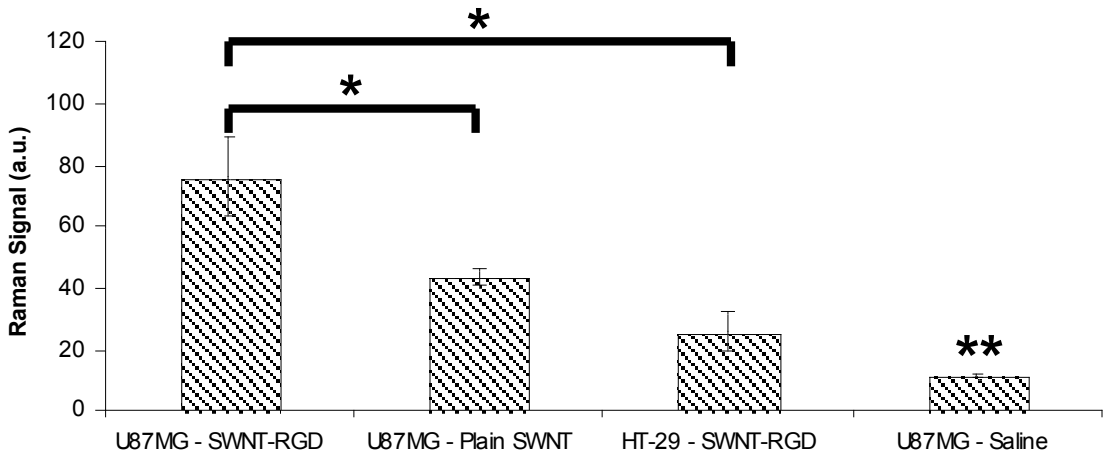

Supplementary Figure 3 SWNT cell uptake studies. U87MG incubated with SWNT-RGD showed 75% higher SWNT signal than control U87MG cells which were incubated with plain SWNT and 195% higher SWNT signal than HT-29 cells which were incubated with SWNT-RGD. " * " indicates $p < 0.05$. U87MG cells incubated with saline only showed significantly lower signal than all groups (" ** " indicates $p < 0.05$ compared to all other groups on the graph).

Theoretical tissue background calculation

The SWNTs used in this study had an absorbance $A = 6.2 \cdot 10^6$ $cm^{-1}M^{-1}$ at 690 nm (measured using DU-640 spectrophotometer, Beckman Coulter). Assuming light absorption accounts for most of the absorbance of the SWNTs, we get that $\mu_{CA}(\lambda,C) = \ln(10) \cdot A(\lambda) \cdot C$, where μ_{CA} and C are the contrast agent optical absorption coefficient and concentration respectively. Upon light exposure I to the absorber at wavelength λ, the absorber will produce a pressure wave $P = \Gamma \cdot I \cdot \mu_a(\lambda)$, where Γ is the Gruneisen coefficient and $\mu_a(\lambda)$ is the optical absorption coefficient of the absorber. The optical absorption (and hence the background photoacoustic signal) of tissues varies between different locations in the body. This variation is due to different amounts of HbO_2, Hb and melanin that leads to different optical absorption characteristics and therefore to

© 2008 Macmillan Publishers Limited. All rights reserved.

different endogenous photoacoustic background signals. We conclude that typical tissues with absorption coefficient of 0.1-1 cm^{-1} will produce a background photoacoustic signal that is equivalent to the photoacoustic signal produced by 7-70 nM of SWNTs.

Importantly, in cases where background signal is mixed with the contrast agent signal (e.g., background cannot be measured prior to contrast agent administration or is not spectrally separated from the contrast agent signal), sensitivity criteria typically requires that the contrast agent signal will be greater than or equal to the tissue background signal. This requirement can be formulated as: $P_{CA} \geq P_{Tissue}$, where P_{CA} and P_{Tissue} are the photoacoustic pressure wave from the contrast agent and the tissue respectively. Assuming the contrast agent does not affect the Gruneisen coefficient of the tissue, this criterion reduces to: $\mu_{CA}(\lambda) \geq \mu_{Tissue}(\lambda)$, where $\mu_{CA}(\lambda)$ and $\mu_{Tissue}(\lambda)$ are the optical absorption coefficients of the contrast agent and the tissue respectively.

Calculation of percentage injected dose per gram of tissue

We have shown that the photoacoustic signal produced by 50 nM of SWNTs is equivalent to the endogenous photoacoustic signal produced by tissues. Since mice injected with SWNT-RGD showed 67% increase in photoacoustic signal produced by tumours, the SWNTs concentration in the tumour can be estimated to be 33.5 nM. The mice were injected with 240 pmol of SWNT-RGD (200 μl at 1.2 μM concentration). Assuming that 1 mm^3 of tissue weights 1 mg, the percentage injected dose per gram of tissue (%ID/g) is therefore ~14 %ID/g.

Comparison to optical fluorescence imaging using quantum dots

We show the superiority of our photoacoustic strategy by comparing it to fluorescence imaging with quantum dots (QDs). We constructed an agar-based phantom with a scattering coefficient, $\mu_s^{-1} = 1$ mm^{-1}, similar to that of tissues and negligible absorption. The phantom had a cylindrical inclusion (4.2 mm in diameter) embedded 4.5 mm below the phantom surface (**Supplementary Figure 4**). The inclusion was filled with a cocktail of plain SWNT and QDs at 200 nM each. The QDs were ~30 nm in diameter with emission wavelength of 800 nm. The phantom was scanned under a fluorescence imaging instrument and under our photoacoustic imaging instrument (**Supplementary Figure 4**).

© 2008 Macmillan Publishers Limited. All rights reserved.

Control inclusions filled with plain SWNT only or QDs only showed no fluorescence signal and no detectable photoacoustic signal respectively. This is likely due to the fact that SWNTs are non-fluorescent at 800 nm (Supplementary Ref. 2). Quantum dots, on the other hand, are highly fluorescent and therefore only minimal energy is available for heating and creating photoacoustic vibrations. The fluorescence image showed a large blurred spot at the center of the phantom, with an estimated diameter of 11.5 mm (full-width half max), whereas the photoacoustic image clearly reveals the edges of the inclusion and accurately estimates it's diameter to be 4.2 mm. Furthermore, the depth of the inclusion was accurately estimated in the photoacoustic image to be 4.5±0.1 mm (data not shown). Depth estimation at this accuracy cannot be done using fluorescence imaging. Additionally, the signal to noise ratio (SNR), which is associated with sensitivity, was significantly higher in the photoacoustic image (SNR = 38) than in the fluorescence image (SNR = 5.3).

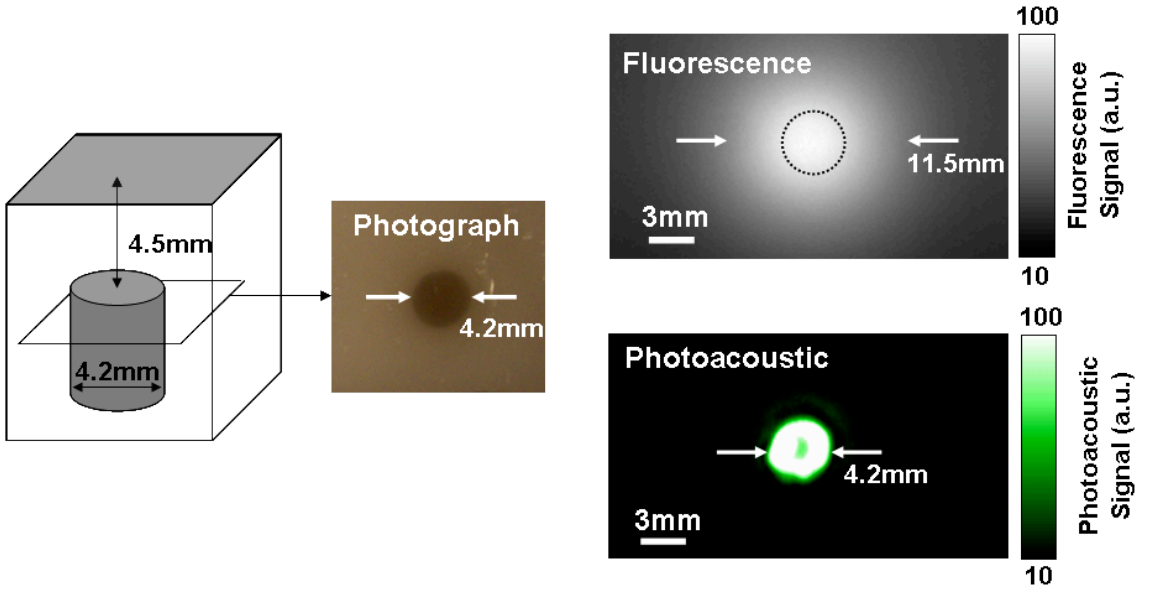

Supplementary Figure 4 Comparison between photoacoustic imaging using SWNTs and fluorescence imaging using QDs. Cylindrical inclusion filled with a mixture of SWNTs and QDs at equal concentrations was positioned 4.5 mm below the surface of a tissue mimicking phantom. Photographic image (right) of a horizontal slice through the phantom illustrates that the inclusion is 4.2 mm across. Fluorescence (top right) and photoacoustic (bottom right) images of the phantom. The dotted circle in the fluorescence

© 2008 Macmillan Publishers Limited. All rights reserved.

image illustrates the real location of the inclusion. The photoacoustic image represents a horizontal slice in the 3D image, 5 mm below the phantom surface. The estimated diameter of the inclusion in the fluorescence image is 11.5 mm (full-width half max) whereas the photoacoustic image accurately estimated the inclusion to be 4.2 mm across.

Supplementary Methods

Tumour *ex-vivo* analysis using Raman microscopy. At the conclusion of every photoacoustic study (4 hr post-injection) the mice were sacrificed and the tumours were surgically removed. The tumours were then scanned using a Raman Microscope (Renishaw Inc.). The microscope has a laser operating at 785 nm with a power of 60 mW. A computer-controlled translation stage was used to create a two dimensional map of the SWNT signal in the excised tumours with 750 μm step size using 12X open field lens. Quantification of the Raman images was performed by using the Nanoplex™ SENSERSee software (Oxonica Inc.) where the mean Raman signal detected from the tumours was calculated.

Mouse arrangement in the photoacoustic system. Female nude mice were used for all the photoacoustic studies. The mice scanned in the photoacoustic system were fully anesthetized using isoflurane delivered through a nose-cone. Prior to the photoacoustic scan, the areas of interest were covered with agar gel to stabilize the area and minimize any breathing and other motion artifacts. A saran-wrap water bath was placed on top of the agar gel. An ultrasonic transducer, placed in the water bath, was therefore acoustically coupled to the mouse tissues. This setup allowed the ultrasonic transducer to move freely in 3D while not applying any physical pressure on the mouse.

Characterization of SWNT photoacoustic properties. We prepared a gel phantom using 1% Ultrapure Agarose (Invitrogen) and 1% intra-lipid (Liposyn II 10%, Abbott Laboratories) to induce scattering into the phantom. We waited 30 min for the solution to solidify and created cylindrical wells 4.2 mm in diameter into the phantom. We then

© 2008 Macmillan Publishers Limited. All rights reserved.

mixed plain SWNT with warm liquid agar at ratio of 1:4 so that the final concentration of the SWNG was 200 nM and poured the solution into the wells. The same procedure was then repeated for SWNT-RGD. After the agar solidified, we covered the wells by another thin layer of warm agar and waited for 30 min for agar to solidify. A complete photoacoustic image of the phantom was acquired at wavelengths between 690-800 nm in 5 nm steps. The photoacoustic signals were compensated for laser power and photodiode response in the difference wavelengths, so that each measurement represents only the inherent photoacoustic signal produced by SWNTs. For image analysis, a 3D ROI was drawn over the SWNT in the phantom and the mean signal in the ROI was calculated.

To test the linearity of the photoacoustic signal as a function of SWNT concentration we used an agar-phantom with no scattering or absorbing additives (i.e. no intra-lipid). SWNTs at increasing concentration were mixed with warm liquid agar in ratio of 1:3 to form SWNTs solutions at 25, 50, 100, 200, 300, 400 nM. Inclusions 3 mm under the phantom surface were filled with the various SWNTs solutions (three inclusions for each concentration, 100 μl per inclusion). A complete photoacoustic image of the phantom was acquired at 690 nm with step size of 0.5 mm. 3D cylindrical ROIs at the size of the inclusion were used to estimate the photoacoustic signal from each well.

Photoacoustic detection of SWNTs in living mice. Plain SWNT at 6 different concentrations were mixed with matrigel (Matrigel Basement Membrane Matrix, Phenol Red-free, Becton Dickinson) at 1:1 ratio creating plain SWNT solutions at 50, 100, 200, 300, 400 and 600 nM. The solutions were then injected subcutaneously (30 μl) to the lower back of mouse (n = 3). After the matrigel solidified in its place (a few minutes) the back of the mouse was scanned under the photoacoustic system. Interestingly, SWNTs at concentration of 200 nM and above had a typical black color. A photoacoustic image with lateral step size of 0.5 mm was acquired using the 5 MHz transducer at 690 nm wavelength. Following the photoacoustic scan, an ultrasound image was acquired using the 25 MHz transducer and the two images were then coregistered. Quantification of the photoacoustic signal was done by drawing a 3D ROI over the inclusion volume that is

© 2008 Macmillan Publishers Limited. All rights reserved.

illustrated in the ultrasound image. The volume of the ROIs was kept at 30 mm^3 (equivalent to the 30 μl that were injected).

Cell uptake studies. We exposed 1.2 x 10^6 U87MG cells to 100 μl of 600 nM SWNT-RGD. As a control, 1.2 x 10^6 U87MG cells were exposed to same volume and concentration of plain SWNT. Another 1.2 x 10^6 U87MG control group was exposed to PBS 1X (PBS pH 7.4 1X, Invitrogen). Additionally, 1.2 x 10^6 cells HT-29 cells were exposed to 100 μl of 600 nM SWNT-RGD (n = 3 in all groups). The cells were exposed for 30 min, and then centrifuged at 12,400 RPM for 3 min. All excess liquid was removed and cells were washed with PBS twice. The cells were then suspended in 15 μl of liquid agar gel and were scanned using a Raman microscope.

Comparison to optical fluorescence imaging using quantum dots. We have prepared a gel phantom using 1% Ultrapure Agarose (Invitrogen) and 1% intra-lipid (Liposyn II 10%, Abbott Laboraties). We waited 30min for the agar-lipid solution to solidify and then created cylindrical wells with diameter of 4.2 mm in the phantom. The wells were then filled with a cocktail of QDs (Qdot(r) 800 ITK™ amino (PEG) quantum dots, Invitrogen), and plain SWNT at equal concentration. Control wells were filled with QDs only and plain SWNT only. Liquid agar was added to all wells at a ratio of 4:1 to allow the well content to solidify. After the dilution with the liquid agar, the concentration of plain SWNT and QDs in the wells was 200 nM. We waited 30 min allowing the agar to solidify and then poured a second layer, 4.5 mm in height, of warm agar-lipid liquid. We waited 30 min and then scanned the phantom in a fluorescence imaging instrument Maestro (CRI). A band pass excitation filter centered around 645 nm and a 700 nm long pass emission filter were used for the scan. The tunable band pass filter was set to scan the fluorescence emission from the phantom at wavelengths between 700 nm to 950 nm. An exposure time of 300 ms was found to maximize the fluorescence signal from the QD-SWNT well while not saturating the camera. Maestro proprietary software was used to calculate the full-width half max (FWHM). SNR was calculated as the maximal signal acquired from the well divided by the average signal in a small ROI drawn 14 mm away from the inclusion's center. We then acquired photoacoustic and ultrasound images of the

© 2008 Macmillan Publishers Limited. All rights reserved.

phantom. The laser wavelength was set to 690 nm and averaging of 16 laser pulses per photoacoustic a-scan was used. The lateral step size was set to 250 μm. The resulting photoacoustic image was analyzed using AMIDE software. The estimated depth of the inclusion was determined by overlaying the photoacoustic image on the ultrasound image which shows the surface of the agar-phantom. The estimated inclusion diameter was measured directly from the photoacoustic image and the image SNR was calculated as the photoacoustic signal at the inclusion area divided by the mean signal outside the inclusion.

The synthesis of QD-RGD that were used in the fluorescence tumour targeting experiment is described elsewhere[1]. The mice were inoculated with 10^7 U87MG cells, and tumours were allowed to grow to 500 mm^3. 200 pmol of QD-RGD were injected via the tail vein to the mice. The mice were imaged 6 hr post-injection using the Maestro (CRI) fluorescence imaging instrument. Excitation filter of 575-605 nm, emission long pass filter of 645 nm and liquid crystal filter range between 650 nm to 850 nm were used for this scan.

Supplementary References

1. Jorio, A., Saito, R., Dresselhaus, G. & Dresselhaus, M. S. Determination of nanotubes properties by Raman spectroscopy. Philos. Transact. A Math. Phys. Eng. Sci. 362, 2311-36 (2004).
2. Barone, P. W., Baik, S., Heller, D. A. & Strano, M. S. Near-infrared optical sensors based on single-walled carbon nanotubes. Nat Mater 4, 86-92 (2005).

© 2008 Macmillan Publishers Limited. All rights reserved.